

# Guided Parafoil High Altitude Research (GPHAR) Flight at 57,122 ft.

Storm Dunker<sup>1</sup>, Joel Huisken<sup>2</sup>, Dave Montague<sup>3</sup>, Justin Barber<sup>4</sup>  
*Airborne Systems North America, Pennsauken, NJ, 08109, United States*

**The purpose of this paper is to summarize the results and document lessons learned following the successful test of a tropopause inflation and flight of a guided parafoil system. The flight was conducted under the NASA Flight Opportunities Program (FOP) on 6 June 2014 from 57,122 ft. MSL using a helium balloon. The total system weight was 224 lb. which flew using a 230 ft<sup>2</sup> parafoil.**

**The primary objectives of the GPHAR program are to both investigate the flight envelope and mature the technology related to the deployment and flight of parafoils at altitudes above 25,000 ft. MSL. Achieving these objectives will enable parafoil systems to be a new viable method for space vehicle recovery.**

**The program had 3 primary technical challenges: 1) successful deployment and inflation of the parafoil system, 2) achieving a stable steady state flight condition, and 3) demonstrating stable and predictable response to AGU control input. Given the lack of precedence of parafoil flight in low density atmosphere, achievement of any one of the three challenges would have been determined a success.**

**During the test, all three challenges were completed successfully. The system successfully released, inflated, and was then controlled with scripted flight followed by autonomous flight. The script portion of flight was a sequence of left and right turns which repeated until transition into autonomous flight at around 12,000 ft. MSL.**

**Data collected during the flight included GPS, inertial, and control data logged onboard the Airborne Guidance Unit (AGU), high definition video, and weather sonde atmospheric data. These data have enabled a number of findings related to high altitude parafoil flight concerning flight performance and turn responsiveness, which will be discussed.**

**In addition to summarizing the test results, this paper will make comparisons of the deployment and inflation data of the 57,122 ft. drop to data collected from an earlier test of the GPHAR system which was conducted at 3,800 ft. MSL. This paper will also evaluate considerations for further exploration of the parafoil flight envelope and make recommendations of future development.**

## I. System Application Background

The GPHAR program is an on-going effort to extend the capabilities of parafoil system technology and mature it to increase the Technology Readiness Level (TRL) of parafoil systems for space recovery or near space recovery applications above 25,000 ft. This ambition requires testing parafoil parachutes in conditions beyond those currently demonstrated. Prior to GPHAR, the highest parafoil inflations and flights are around 30,000 – 35,000 ft. MSL, and are not widely documented, exception being Fields, who experienced only partial successes<sup>1</sup>.

Traditional options for space access systems are no recovery (e.g. many 1<sup>st</sup> stage rockets) and ballistic parachute recovery (Shuttle Solid Rocket Boosters, Apollo & Soyuz capsule) which offers some re-use. The items recovered using ballistic parachutes are logistically challenging and expensive to recover and retrieve due to remote landing areas or ocean landings. The use of parafoil systems for space or near space recovery promises huge recurring

<sup>1</sup> Parachute Systems Engineer, Airborne Systems, 5800 Magnolia Ave, Pennsauken, NJ 08109, AIAA Member.

<sup>2</sup> Parachute Systems Specialist, Airborne Systems, 5800 Magnolia Ave, Pennsauken, NJ 08109.

<sup>3</sup> Software Engineer, Airborne Systems, 5800 Magnolia Ave, Pennsauken, NJ 08109.

<sup>4</sup> Parachute Systems Engineer, Airborne Systems, 5800 Magnolia Ave, Pennsauken, NJ 08109.

savings for the space access industry. Benefits include improving re-usability of launch vehicles, reduction in recovery logistics made possible by precision guided landings, reduced parachute system mass and volume over ballistic systems, and potentially reduced parachute system cost.

A key enabler of the capability is the maturity of precision guided parafoil systems, which have been developed over the past 15 years for military aerial delivery applications. Precision Aerial Delivery Systems (PADS), have been rigorously tested and used operationally for payloads up to 10,000-lbs and 25,000-ft MSL, and as much as 42,000-lbs has been demonstrated.

## II. Test Approach

Since the NASA Flight Opportunities Program is essentially a near space access provider, it imposed no formal requirements for the test objectives or overall program method, other than some mission safety requirements and the requirement that the research shall elevate the TRL for a value adding capability. Rather, the technical requirements, objectives, and mission operations were tailored to values and desired capabilities which Airborne Systems thought would advance the TRL and which were formalized in a proposal to NASA.

### A. Objectives

The self-declared challenges and thus primary technical objective for the GPHAR test included 1) deploying a parafoil in very low density atmosphere, 2) achieving steady state forward flight, and 3) demonstrating stable and predictable response to AGU control inputs, while simultaneously collecting flight data during these events. Several secondary objectives were also identified related to fundamental matters of scientific interest for parafoil systems, including:

- At what density does it become difficult to maintain L/D for parafoil parachutes
- At what density does it become difficult to maintain effective control over parafoil parachutes
- What scaling guidelines are appropriate for stroke commands vs. altitude
- What is the effect of reduced added mass on flight performance and turning (contained and entrained air mass is reduced)
- What is the maximum altitude / minimum density which would be reasonable for parafoil recovery applications

### B. Design of Test

For the next step in expanding the parafoil flight regime, Airborne Systems selected a sliderless static line deployment from an altitude of 50,000 to 60,000 ft. MSL, which for the provided balloon, was 224 lb. of lifted mass. To support this, an existing 230 ft<sup>2</sup> personnel parafoil was custom modified and a low-temperature low-pressure capable Airborne Guidance Unit (AGU) system was designed and built. These components are identified in Figure 1.

The anticipated flight time was > 40 minutes. During this time, it was desired to perform flight activities which would be useful for understanding the new environment. AGU software was designed to command a series of 4 programmed strokes vs. time that would essentially repeat in a loop. This design of repetitive controlled inputs would show trends in steady flight, turn, and stability performance over a wide range in altitude.

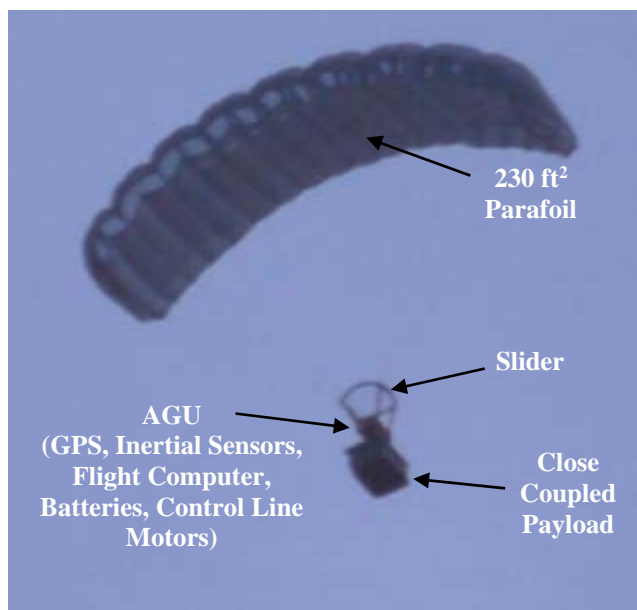


**Figure 1. GPHAR System Components (Slider not used in high altitude flight)**

The planned nominal mission profile included:

- 1) Steady ascent to a targeted 55,000 ft. MSL
- 2) Prompt release to avoid dwell times and to make efficient use of camera and AGU battery life
- 3) Static line deployment
- 4) Canopy inflation (no slider)
- 5) Accelerating to steady state flight
- 6) Release deployment brakes
- 7) Perform scripted turn commands (programmed stroke commands vs. time)
- 8) Exit scripted turns at 12,000 ft., enter autonomous navigation to pre-programmed landing waypoint
- 9) Radio Control intervention as necessary for safety
- 10) Optional Flight Termination System (FTS) activation (round canopy) for ballistic landing
- 11) System landing and recovery

An example simulation of the ascent / descent trajectory overlaid on Google Earth is shown in Figure 2.

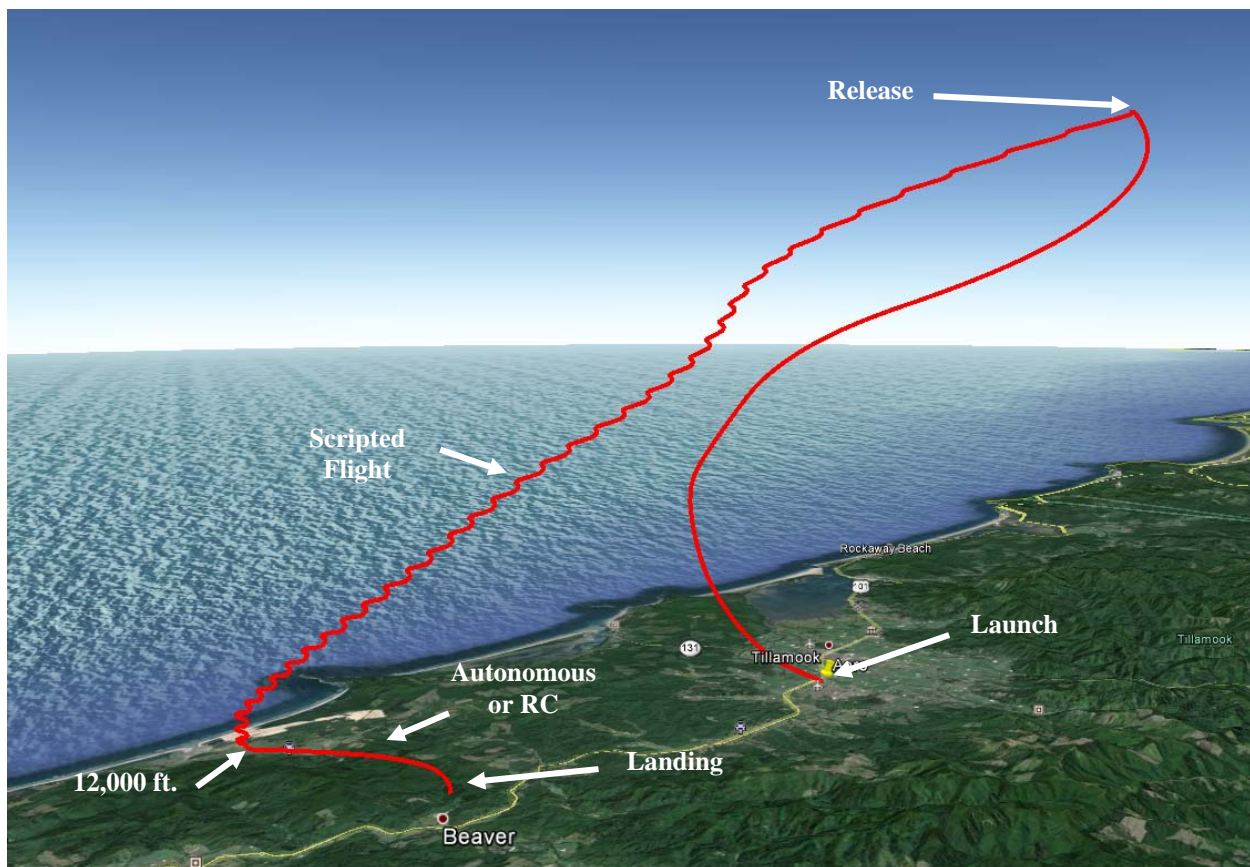


**Figure 2. Example GPHAR Trajectory**

The logistics, planning, safety, and conduct of the test itself, as well as lessons learned, are not intended to be a part of the subject paper. This paper takes focus of the Ram Air performance results.

### C. Selection of Canopy Size

The use of wing loading, known as  $W/S$  (lbs/ft<sup>2</sup>) and calculated as combined suspended weight and canopy weight divided by average of top and bottom skin surface area, can be used as a scaling mechanism in which to size a parafoil parachute over a moderate range of masses, when base performance of similar planform is known (e.g. L/D and descent rate). This method allows selecting a parachute size for a given payload mass to meet a required Rate of Descent (ROD) (or forward or total velocity) at a target altitude, which, for space recovery applications, is anticipated to be an ROD of under 15 ft/s at touchdown, presumably within 5000 ft. of sea level. A further anticipated requirement is that the canopy should be able to effectively navigate and penetrate ground winds.

For the 224 lb. GPHAR mass, a 230 ft<sup>2</sup> parafoil was selected based on the existing Airborne Systems Intruder planform design. This planform design had been selected by the U.S. Army for the Military Freefall Advanced Ram Air Parachute System (RA-1) and was well understood. The corresponding wingloading of 0.97:1 would be expected to descend at approximately 10 ft/s at sea level without control inputs, and would be capable of penetrating winds in excess of 30 ft/s. It is noted that the planform type was selected primarily since it had a well-known performance dataset when used on PADS.

#### D. Design of Control Inputs

An increase in turn responsiveness, specifically turn rate for a given stroke amount, has been observed on multiple planforms and sizes at higher altitudes up to 25,000 ft. MSL. For a similar precision delivery system planform to the one used by GPHAR, reduced command strokes are routinely used at higher altitudes for a given suspended weight to compensate for increased turn responsiveness. Still, the effect of density altitude on canopy control at the planned tested altitudes is uncertain, and is thus a major concern for the design of test.

This concern is also similar to the phenomenon which occurs at higher wingloadings. Parafoil response to control inputs is known to increase as the wingloading on a particular parachute is increased. This requires that strokes be decreased as a function of weight.

A common thread between both of these phenomenon is that with increased Kinetic Energy, turn responsiveness is increased and reduced strokes are required.

As turn rates elevate, risk of diving or spiraling turns also increases, which increases descent rate, payload accelerations, and the complexity of providing effective GN&C through the AGU. It was logically assumed that flights conducted above this altitude regime would experience further trends of increased sensitivity.

##### i. Mass Ratio

Due to concerns of control inputs and general stability at high altitudes, the mass ratio ( $R_m$ ) concept was investigated for suitability into stroke scaling.

A ram air parachute system is really a simplified two body system; a payload of a mass that does not vary with altitude and a canopy mass that does. It is reasonable to consider that a ratio of masses that is dependent on density could somehow be useful to explain differences in behavior of a ram air parachute in flight at different altitudes. Since it is the canopy that provides control over the system, any change to its Moments of Inertia (MOI) is logically a potential source in behavior response change. Specifically the question for GPHAR was what strokes should be used to make turns as a higher altitudes.

For the purposes of GPHAR, the conventional round parachute mass ratio was used as a starting point<sup>4,5,6</sup>. The mass ratio is a unitless term composed of density, payload mass, and drag area variables. The traditional definition of mass ratio for round parachutes is commonly expressed as:

$$R_m = \frac{\rho * (Cd * S)^{3/2}}{M} \quad (1)$$

Where:  $\rho$  = Density  
 $Cd$  = Drag Coefficient  
 $S$  = Canopy area  
 $M$  = Mass of payload plus parachute

For round parachutes, the upper term in the ratio could be considered to be the effective air mass of the internal volume and entrained air mass following the canopy, as it is dependent on the canopy diameter and generally approximates the volume of a sphere of the size of the nominal diameter,  $D_o$ . The presence of the  $Cd$  term adjusts the ability of the canopy to contain this air mass, where canopies with more geometric porosity and thus lower  $Cd$  have a reduced ability to hold air mass. Since the GPHAR mission involves a parafoil, which has a much smaller area and internal volume than a round canopy for similar payload weights, and since the volume of contained air

inside is fixed without geometric porosity, the upper term becomes an ineffective way to calculate internal volume air mass.

Since the volume is known,  $R_m$  could be written simply as

$$R_{m\text{parafoil}} = \frac{\rho * \text{Volume}}{M} \quad (2)$$

This ratio results in a comparison between an upper mass, located at the canopy, and a lower mass, located at the payload, which could affect the steering responsiveness of a canopy, specifically yaw or roll motion of the parafoil wing. In the view of yaw or roll rotations, the MOI is highly relevant, and the MOI of a canopy and contained air mass, if allowed to rotate more freely, could potentially affect steering responsiveness. However, if MOI's are really to be key to steering stability, and mass ratio a mechanism to characterize this, the mass of the parafoil canopy should be removed from the bottom term and added to the upper term, resulting in:

$$R_{m\text{parafoil}} = \frac{\rho * \text{Volume} + m_{\text{parafoil}}}{m_{\text{payload}}} \quad (3)$$

This ratio now expresses a comparison between a simplified two mass system with one mass at the canopy (parachute + air) and a second at the payload.

The practical benefit of mass ratio to GPHAR was that risk reduction drop tests could emulate the actual mission mass ratios by conducting drop tests at relatively low altitudes using payload weights in excess of the planned missions' 100 kg. It was predicted that steering controls found to be appropriate for the GPHAR canopy at the heavier wingloadings in lower atmosphere would also be appropriate steering controls at the same mass ratios in the upper atmospheres at the nominal wingloading. This approach would allow selection of maximum stroke to be used at the maximum altitude expected during the test.

Using the selected maximum stroke at maximum altitude, a stroke scaling law was implemented for the GPHAR drops which would scale the stroke according to the density at the relevant flight altitude at the time of stroke command. It was determined to be appropriate to use just density as the scaling variable since both volume and  $M_{\text{RAMAIR}}$  and  $M_{\text{PAYLOAD}}$  masses were constants throughout the flight.

However, the mass ratio term is an imperfect solution to a complicated problem. It oversimplifies stroke turning responsiveness which is actually dependent on more variables than just the mass at the canopy. Complex aerodynamic and physical relationships exist in addition to the change in mass. A huge impact to turn responsiveness is potentially Kinetic Energy. Simply put, at higher altitudes, and even at higher wingloadings, Kinetic Energy is much higher, due to a square law. It will therefore take more force, or the same force over a longer period of time, to effect a given turn and change the direction of travel of the payload mass. The above mass ratio approach was cautiously used based on its principle dependency to density, and for lack of a better model.

## ii. Kinetic Energy vs Altitude

Since Kinetic Energy increases with the square of velocity, there is anticipated to be a large difference in flying KE throughout the flight altitudes. The concern for an impact to control responsiveness is based on the premise where the available force to control the system (initially) stays the same while the force-magnitude or force-duration required to control the system increases greatly for a given turn.

A parafoil flying straight can be simplified as having a single lift vector located above the center cell at the quarter chord. Banking that vector via roll, using steering inputs, will change the payload trajectory, and thus heading. Since the lift vector can be assumed to be a constant force at a given airspeed and density, the magnitude of the lift vector is the same for all altitudes, regardless of system Kinetic Energy.

Control inputs also manipulate the airspeed by increasing descent rate and / or diving, which would increase the magnitude of the lift vector.

Among other things, the ability of the lift vector to change the direction of travel of a payload depends on the banking and change of airspeed. The difference in the GPHAR payload at steady state kinetic energy across the altitude range is shown in the figure below.

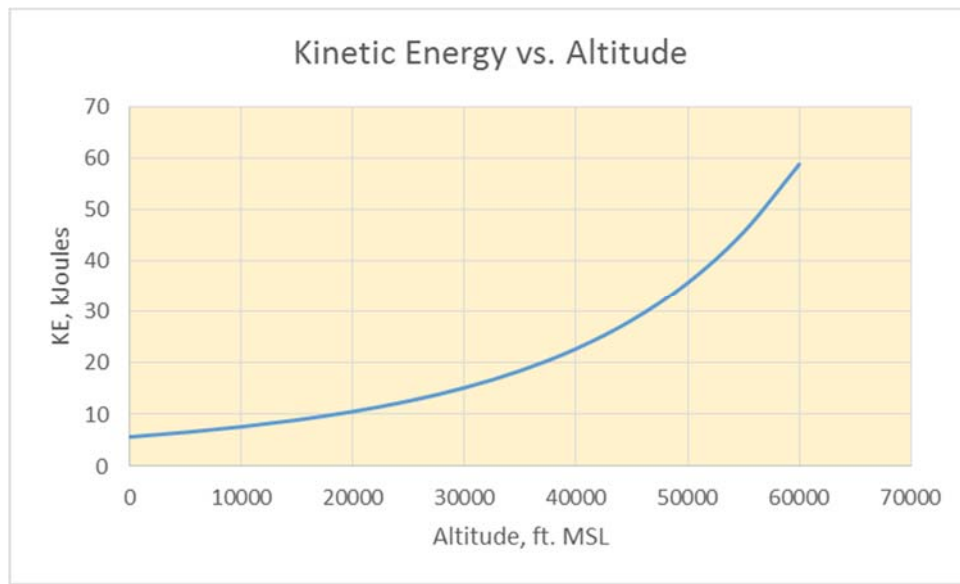


**Figure 3. Plot of KE vs. Altitude of GPHAR**

As can be seen, there is 9 times more kinetic energy in the system at 55,000 ft. than at sea level.

In practice, as a result of this concern, a small margin of safety was added to the strokes scaling law by way of fewer inches of stroke in an effort to be conservative. As a result of both the mass ratio review and the kinetic energy review, the maximum amount of stroke for 55,000 ft. MSL was selected for the flight, termed L<sub>255,000</sub> and R<sub>255,000</sub> for left and right turns respectively.

### iii. Scripted Flight

The planned scripts included stroke commands which loop, allowing the observation of differences in control performance as a function of altitude / density. A period of straight flight was planned between turns to let the system achieve stable flight before beginning the next. Turns to the left and right would be made, and then turns of two different stroke inputs would be made. Steps 3-10 in Table 1 represent one loop (72 seconds). L1 and R1 are about half the stroke of L2 and R2, respectively.

Step	Step Duration (seconds)	L	R
1	exit	Brake Setting	Brake Setting
2	20	Base Stroke	Base Stroke
3	8	<b>L1 Stroke</b>	Base Stroke
4	10	Base Stroke	Base Stroke
5	8	<b>L2 Stroke</b>	Base Stroke
6	10	Base Stroke	Base Stroke
7	8	Base Stroke	<b>R1 Stroke</b>
8	10	Base Stroke	Base Stroke
9	8	Base Stroke	<b>R2 Stroke</b>
10	10	Base Stroke	Base Stroke
REPEAT from 3			

Table 1. Scripted Stroke Time Table

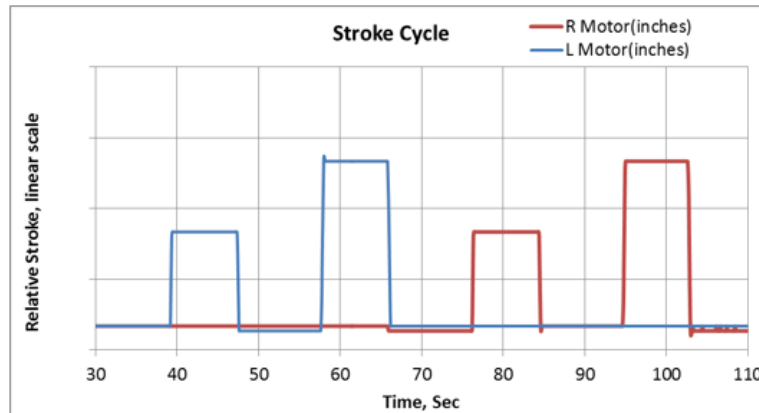


Figure 4. Example Script Stroke Cycle

The baseline deflection of both control surfaces during straight flight was set to remove slack from the rigging of the system. This also helps eliminate adverse yaw characteristics of parafoils that can occur at low trailing edge deflections when initiating a turn. The strokes for two types of turns were calculated. “L1” turns used a smaller stroke which are intended for a small course correction. “L2” turns are larger stroke, maximum rate, maneuvers used to make large course corrections (i.e. > 90 degrees). These are the basic types of turns that are utilized by the autonomous guidance software.

### iv. Stroke Scaling

The amount of stroke of each of the inputs L1, L2, R1, and R2, were scaled non-linearly based on altitude, according to the relative pressure (pressure at altitude / pressure at sea level), which approximates similar changes in density sufficiently for this purpose. This method was chosen since it utilized existing metrics within the flight software and required a minimum of new programming.



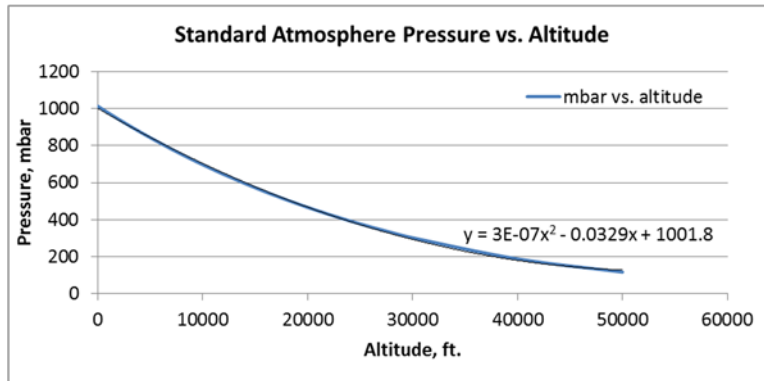


**Figure 5. Standard Atmosphere Pressure**

Given that the maximum stroke at full altitude, assumed to be 55,000 ft., is known, it was then pertinent to identify the maximum stroke at low altitude. For altitudes 12,000 ft. and below, the standard value for the autonomous PADS flight software for this parafoil was used, termed  $L2/R2_{12,000}$  and  $R2_{12,000}$ . The difference between  $L2/R2_{55,000}$  and  $L2/R2_{12,000}$ , shall be termed  $\Delta L2$  and  $\Delta R2$ , respectively. Similarly, the stroke values for  $L1$  and  $R1$  are correspondingly termed  $\Delta L1$  and  $\Delta R1$ .

The scaling algorithm used was then based on the pressure best fit polynomial with adjustments for the mbar range expected and factored against the  $L1$ ,  $L2$ , and  $\Delta$  terms using the algorithm:

$$Stroke_{L1} = L1_{55,000} + \frac{\Delta L1 * (3.0E^{-7} * Z_{MSL}^2 - .0329 * Z_{MSL} + 895)}{596} \quad (4)$$

$$Stroke_{L2} = L2_{55,000} + \frac{\Delta L2 * (3.0E^{-7} * Z_{MSL}^2 - .0329 * Z_{MSL} + 895)}{596} \quad (5)$$

$Z_{MSL}$  is altitude above mean sea level in feet. Stroke  $R1/R2$  terms are similarly calculated.

The selection of stroke inputs were intentionally over-conservative with the intent to minimize the potential of inducing an unrecoverable dive in a maneuver which would both compromise the safety of the flight as well as preclude the collection of valuable flight data.

The maximum stroke settings for the autonomous flight, that under 12,000 ft., was fixed so that the system would operate within the known input-response regime.



### E. Attenuation Design

High altitude balloon release events involve starkly different deployment dynamics when compared to lower atmosphere deployments. For example, when a payload with a packed parachute is released from a balloon, the payload falls as the lines unstow, which eventually snatches out the parachute from the deployment bag. The lines act as both a connection to the payload, whereby conservation of momentum must be considered, but also they act as a spring, creating a recoil of the parachute toward the payload. If unabated, the parachute could descend faster than the payload for a short period of time (seconds), during which no control over the lines or canopy is maintained, posing a great risk of entanglement or other malfunction. At lower altitudes, this phenomenon is not as easily observed since the denser air easily dampens the parachute's recoil.

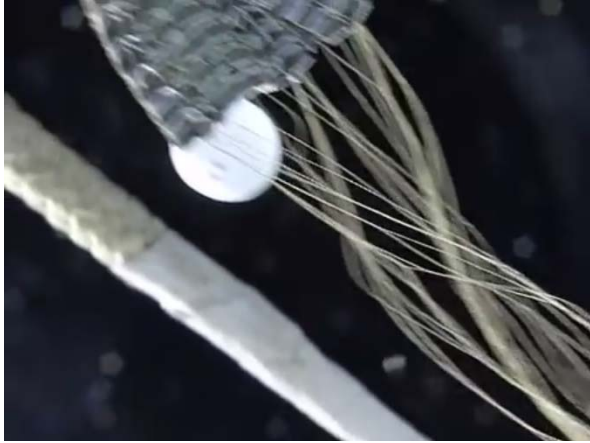


**Figure 6. Example Parachute Recoil after Line Stretch**

An example of an uncontrolled parachute just after line stretch can be seen in an ExoMars static line release test (Cambridge University publicly available video). The host balloon is still in the video image, Figure 6, representing the vertical axis from the camera point of view.

The deployment of the GPHAR canopy was therefore designed to utilize an attenuation strip of calculated rip strengths for a prescribed drop distance. The below plot shows the predicted distances of payload and canopy (parafoil), their relative velocities, and the effect of with and without attenuation on the delta distance between the parafoil canopy and payload. This model assumed a static balloon position during release for simplicity, and zero air resistance.

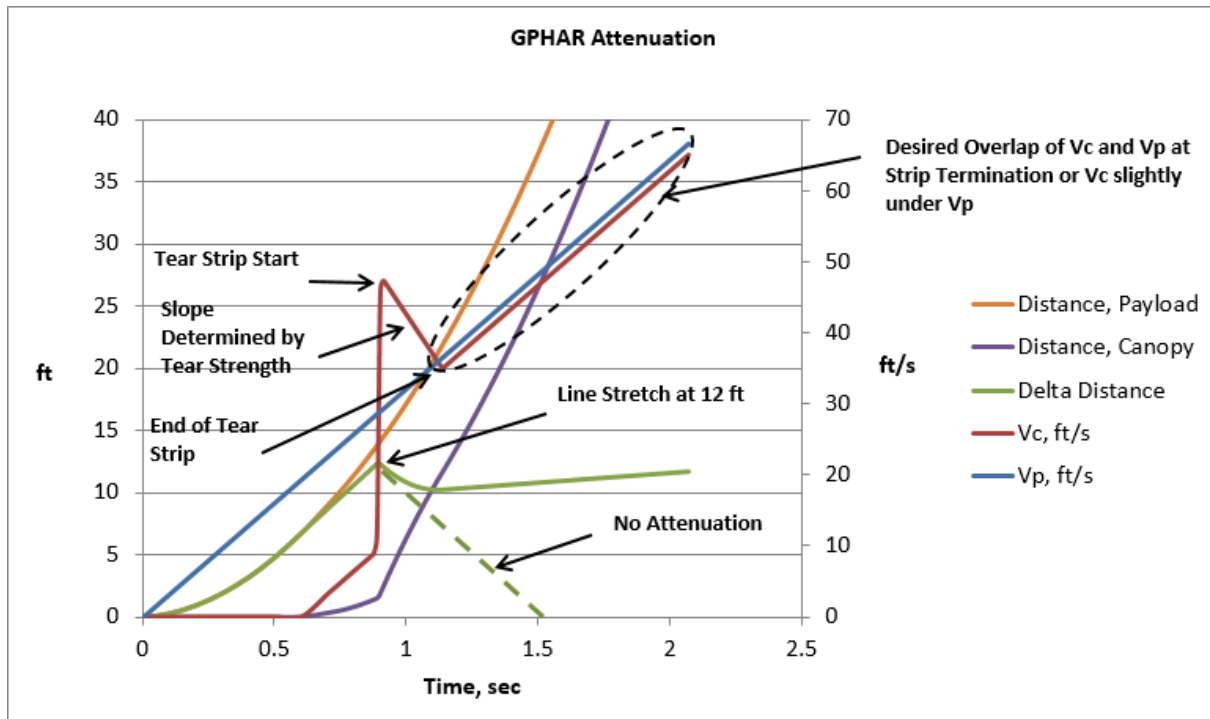


**Figure 7. Attenuation Design**

An objective of the attenuation design was to achieve a theoretical canopy velocity ( $V_c$ ) that matched the payload velocity ( $V_p$ ). The attenuation strip itself was designed to release at the canopy end so as to not trail anything that could entangle with the lines.

## F. Technical Risks

In expanding the capabilities of parafoil flight, risks are naturally present in the form of excursions beyond the previously demonstrated envelope. Risks identified for the GPHAR program included, at minimum:

- Lower air density
  - Reduced ability for thermal exchange by air
  - Unknown impacts from new apparent mass and mass ratios
- Lower air temperature
- Overall canopy stability and turn responsiveness
- Canopy rebound after release and deployment
- Higher air speeds
- Higher kinetic energy in steady flight

To improve chances of success, mitigating actions were taken to reduce technical risk.

### i. Canopy Modifications

As a result of the low air density environment, concern was present regarding the timely inflation of the parachute after release. Consequently, bottom skin vents were added to the test canopy. These vents have been used previously to improve inflation reliability in PADS systems previously, as well as in Building Antenna Span Earth (BASE) jumping canopies.

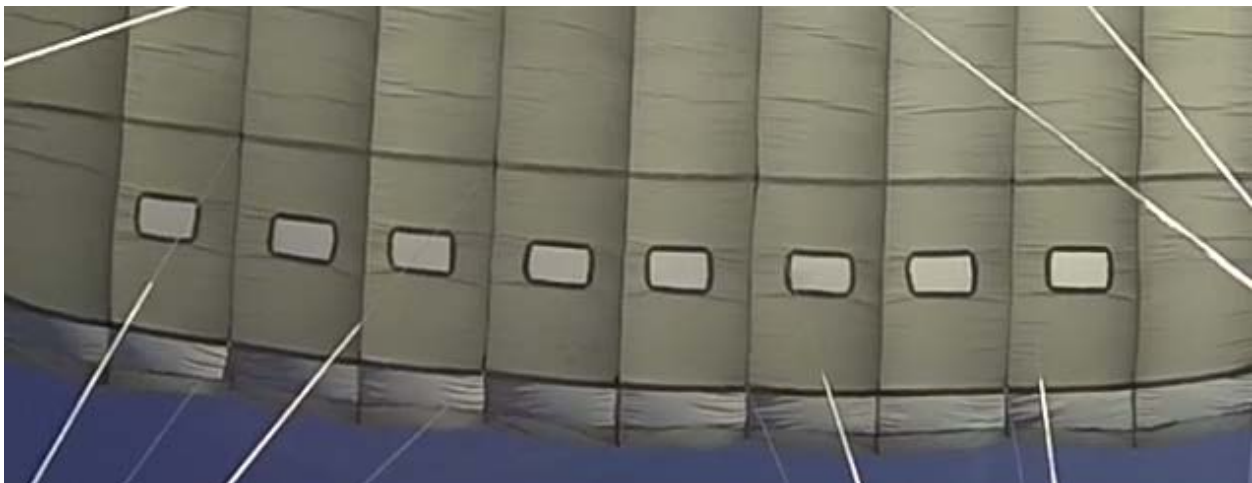


**Figure 8. Bottom Skin Vents**

### ii. AGU Configuration and Adaptations

One of the greatest uncertainties was the expected parafoil flight performance and overall stability, especially in response to turn inputs. Of the conceived extremes of stability issues, there could have been any of the following: a propensity to enter line twists, to enter a spinning dive, to stall, and other less easily described instabilities.

In an effort to combat these stability issues, the Airborne Systems Aero AGU, used as a baseline, was re-configured for close-coupling attachment to the payload, making a 2-body system, instead of a normal 3-body system where the payload is suspended. The 2-body system restricts the freedom of motion between the bodies and also allows a higher payload CG, which is generally considered more stable / recoverable. These changes are not always desirable in all PADS applications for various reasons, but for the short term goal of expanding parafoil capability, they were considered risk reducers.

The survivability of electronics at cold temperatures, the reliability of the power supply, and the potential overheating of internal electronic components due to poor transfer of thermal energy into air were also strong concerns for the AGU. A number of environmental and duty cycling tests were performed, including simultaneous motor movement tests of an expected mission at cold temperature. In preparation of this environment, or as a result

of lessons learned, the batteries were substituted, a thermal control system was designed, a new avionics board was designed, and motors were exchanged for brushless, greaseless variants.

### iii. Prior testing

Multiple drop tests were performed in preparation of the balloon release. Drop tests were performed to verify deployment configuration. In these tests, the GPHAR system used a large round parachute as the host platform and then released allowing the verification of the unreefed static line deployment. The mesh slider present in Figure 9, which was installed for other purposes on other drops, was packed down (disreefed).



**Figure 9. Deployment Testing at 3,800 ft. MSL**

Many further drop tests were performed to investigate the stroke envelope. Attention was paid to stroke envelopes, stroke scaling with altitude, mass ratios. Although the relevance of mass ratio for parafoil parachutes was questioned since parafoil parachutes have such little internal volume relative to round parachutes, the uncertainty in parachute behavior at higher altitudes persuaded further investigation. Notably, other high altitude balloon drop tests have seen instabilities at certain altitudes due to density, example being experience observed in testing of Mars guided parachute<sup>2</sup>, which had a round canopy experience severe coning instability until a more stable density was achieved (potentially).

Since drop testing at higher altitudes is more costly, and limited to unpressurized aircraft, all drops were done in relatively dense atmosphere (<12,000 ft. MSL). As a result, drops were performed at different weights to target similar mass ratios as would be experienced in the balloon test.

An important philosophy for the selection of strokes, for test, and for application, is to avoid making turns which cause unstable behavior. This can be mitigated by selecting lower strokes held for a longer time to achieve target headings. This led to fairly conservative stroke settings, which still resulted in some surprises.

## III. Test Configuration

The configuration is summarized as follows:

<b>Launch Site:</b>	Tillamook, Oregon
<b>Total Drop Weight:</b>	101.6-kg (224-lbs)
<b>Total Parachute Weight:</b>	27.4-kg (60.3-lbs) Includes main canopy, airborne guidance unit (AGU), and flight termination system (FTS).
<b>Ascent and Float Time:</b>	45-60 minutes
<b>Flight Profile:</b>	<ul style="list-style-type: none"> <li>• Flight Characteristics Scripted Maneuvers from release to 12,000-ft MSL</li> <li>• Autonomous Flight from 12,000-ft MSL</li> <li>• Optional low altitude flight termination if needed for safe landing</li> </ul>
<b>Ram Air Parachute:</b>	230-ft <sup>2</sup> Intruder™ semi-elliptical planform
<b>Airborne Guidance Unit:</b>	Aero v2-500 SN001, v3.8.11f Flight Software

A photograph of the flight train in the prelaunch configuration is shown to the right. The drop configuration included multiple redundant radio communications systems between the balloon, payload, AGU, and the mission control station at the launch site as well as an airborne and a ground-based recovery team. Two payload-mounted GoPro® cameras were used to capture test video.

The AGU included a thermostatically controlled battery heating system. This battery configuration was environmentally tested in a laboratory to help ensure it would function over the ascent and descent to/from an altitude of 100,000-ft MSL, which is beyond the requirement for the GPHAR test.

The planned flight profile requires wind conditions that preclude the possibility of the system from landing in populated areas, or over-flying at low altitude. Mission planning and profile simulations were performed jointly by AS and NSC leading up to the test event to ensure that the wind conditions were acceptable for the execution of a safe flight test.

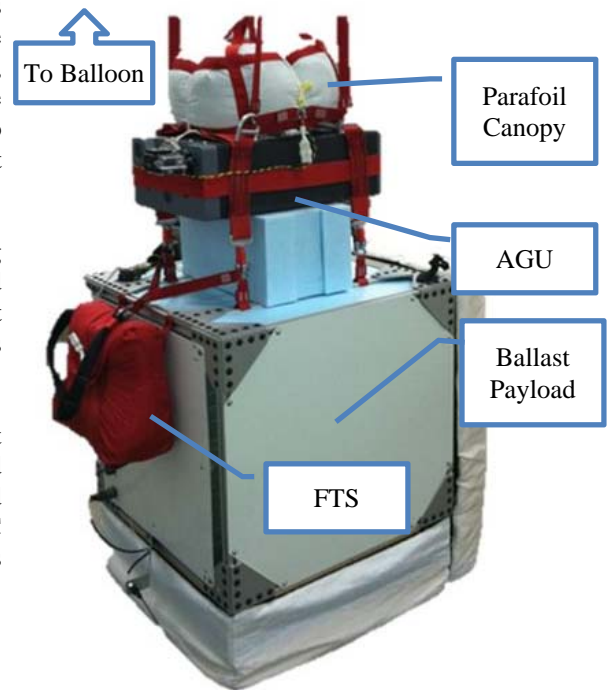


**Figure 10. Deployment Train**

#### IV. Results

The balloon launch was conducted under nominal conditions from NSC's Operations Command Center (OCC) at Tillamook airport. The balloon ascended at a nominal rate of 1200-ft/min and reached 55,000-ft in approximately 47 minutes, and was then released.

However, radio communications between the AGU and OCC were lost after an anticipated loss of line-of-sight with the payload during the ascent. Release of the parachute system from the balloon was commanded from the OCC as planned at 55,000 ft. MSL. Streaming video showed a good deployment of the main canopy. By all standards, all three test objectives were achieved; inflation, steady state flight, and scripted turns, with a full flight log.

A total of 29 script loops were achieved prior to the 12kft MSL switch to autonomous navigation. The total flight time was approximately 52 minutes, inclusive of some diving turns above 40,000 ft. MSL.

Visual and radio communications between the AGU and recovery teams was lost until the Airborne Systems team made visual contact at approximately 4,000-ft AGL. The system was monitored from this point. The system was correctly on an autonomous trajectory with a bearing in the direction of the launch site. The flight termination was activated by the airborne recovery team member at 1000-ft AGL over a safe landing area, as planned. The parafoil canopy flight was arrested and the system landed softly under the ballistic flight termination parachute in a farm field.



**Figure 11. I230 in a Commanded Turn**

Recovery of the onboard flight log and high definition GoPro® cameras indicate



that the flight profile was autonomously executed as planned and that flight performance data of the scripted maneuvers was recorded. The data is continuing to be analyzed to characterize the dynamics of the ram air canopy at high altitude and make adjustments to the autonomous canopy control scheme for subsequent flights. Data indicates that the AGU battery heating system functioned as designed internal temperatures and performance of the actuation system was within expectations.

### A. Day of Test Conditions

Prior to the GPHAR launch, a weather sonde balloon was launched to provide both temperatures and wind profiles. The AGU itself also served as a weather balloon on the ascent, also measuring GPS position and altitude. It is assumed the balloon did not glide and had a ballistic ascent.

The temperatures of ascent and descent are shown in the below plot. The smoothness of the temperature on the descent is due to much higher rate of descent than ascent (reduced dwell time). This terminates part way down due to unknown reasons.

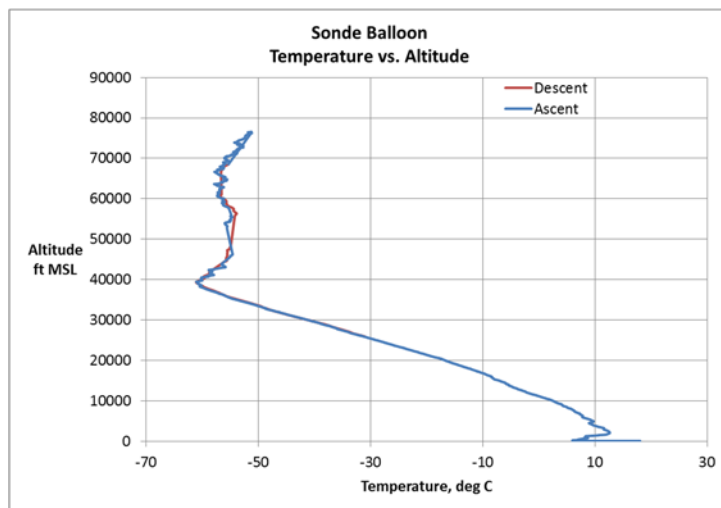


Figure 12. Temperature vs. Altitude

The observed wind heading and magnitudes during ascent are assumed to be true observations and require no reduction or post processing. This is the preferred wind source to use during flight performance data reduction.

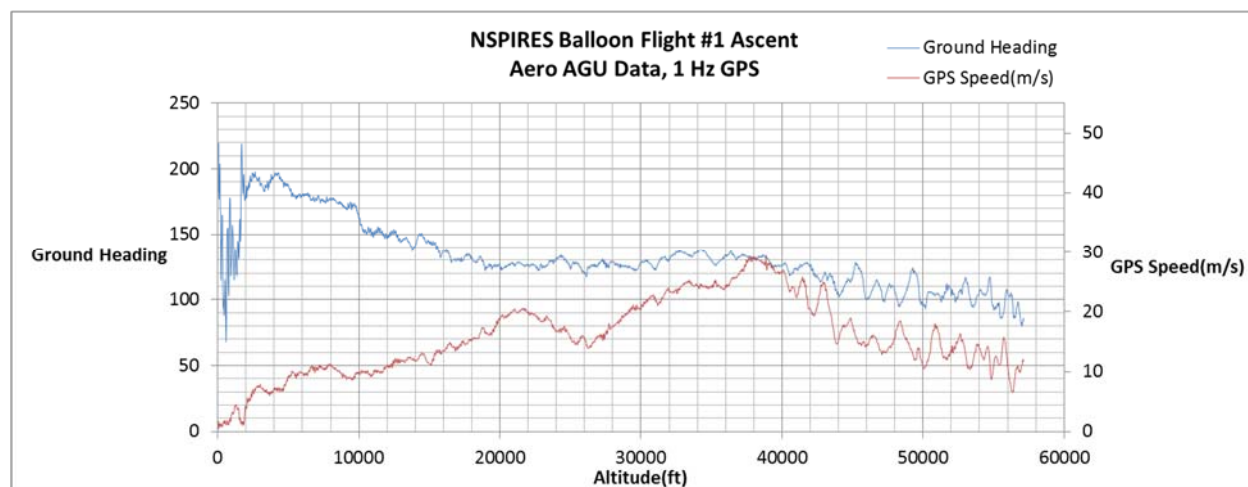


Figure 13. Ascent Data

## B. Trajectory

The complete ground track of the ascent and descent covered approximately 78 km, with a trajectory of approximately southeast. Launch occurred at 36 ft. MSL and landing at 800 ft. MSL. In the figure below, the yellow track represents the ascent, the white track the descent, and the red track the autonomous portion.

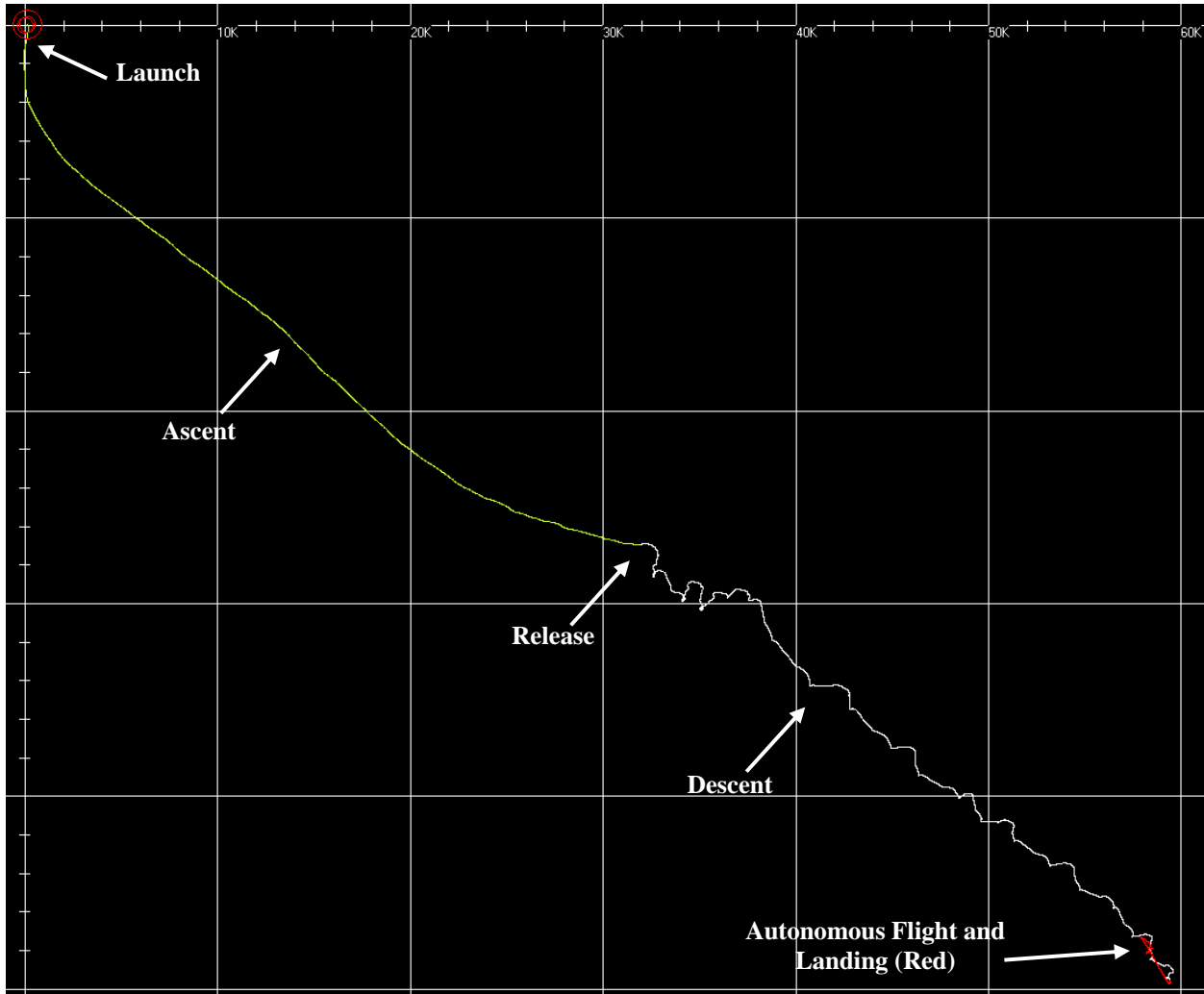
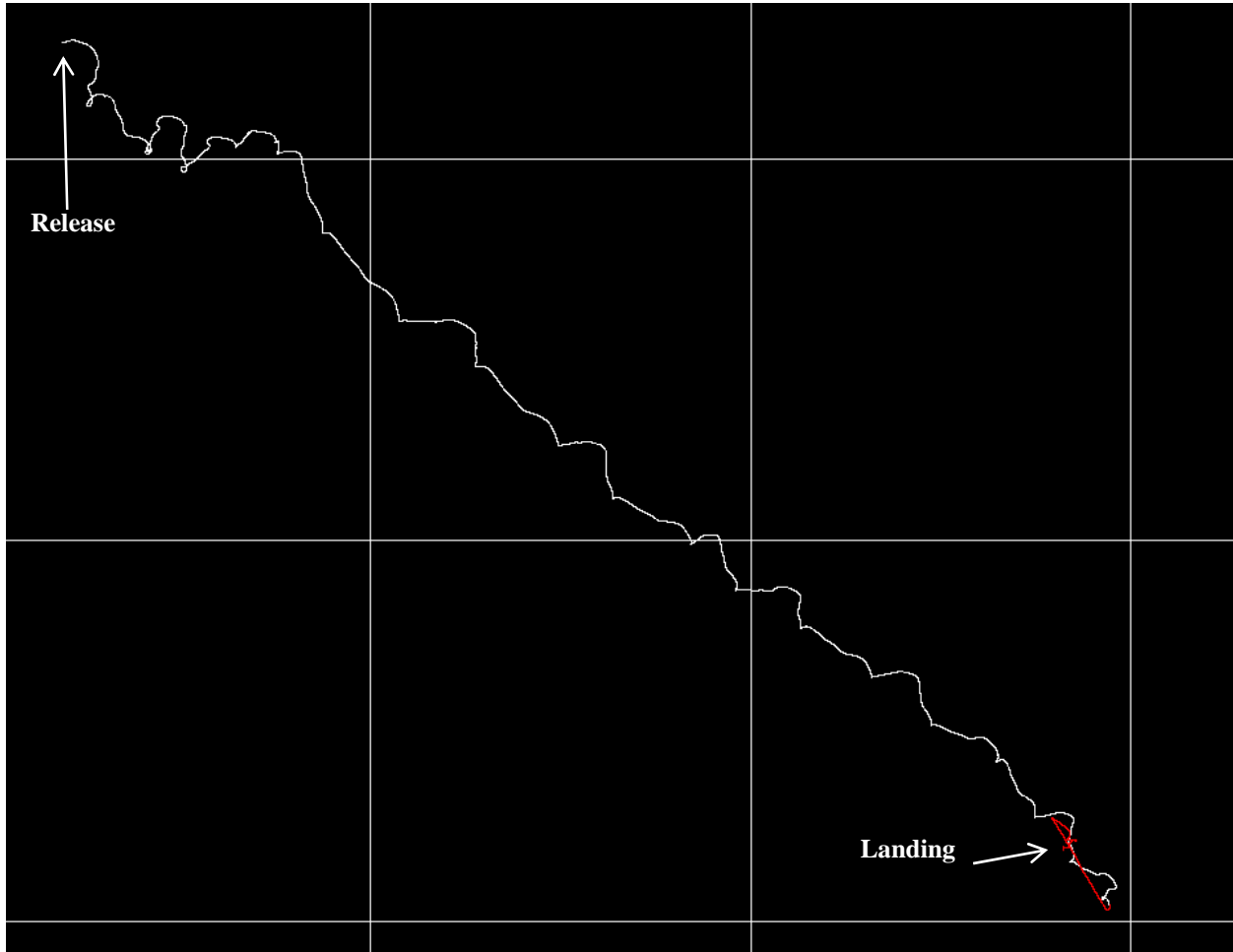


Figure 14. Ground Track of Ascent and Descent

### C. Flight Trajectory

The flight trajectory is shown below with scripts in white and autonomous in red. The quadrants are 10 km square. The balloon release occurs in the upper left corner. As can be seen, the flight pattern is more chaotic in the initial stages of flight, and includes some 360 loops. This would be expected in turns with higher turn rates. The trend observed shows that the higher altitude turns were more sensitive / responsive even though less control stroke was used.



**Figure 15. Flight Trajectory**

As with many parachutes, a small turn bias may be experienced even in a neutral control position. The GPHAR system experienced a right bias for the duration of the flight, which caused more responsive right turns than left turns.

The red autonomous section includes both autonomous flight in the direction of the launch site, but also the portion of flight with descent under the flight termination system, which was activated at about 1,000 ft. AGL.

High winds were experienced below 5,000 ft. MSL. However, landing occurred with much lower wind.



The descent was of about 52 minutes in duration. Touchdown occurred at approximately 750 ft. MSL. The descent time could be expected to be about 7 minutes longer if only essential turns were commanded and if slower turns were utilized, as would be in application.

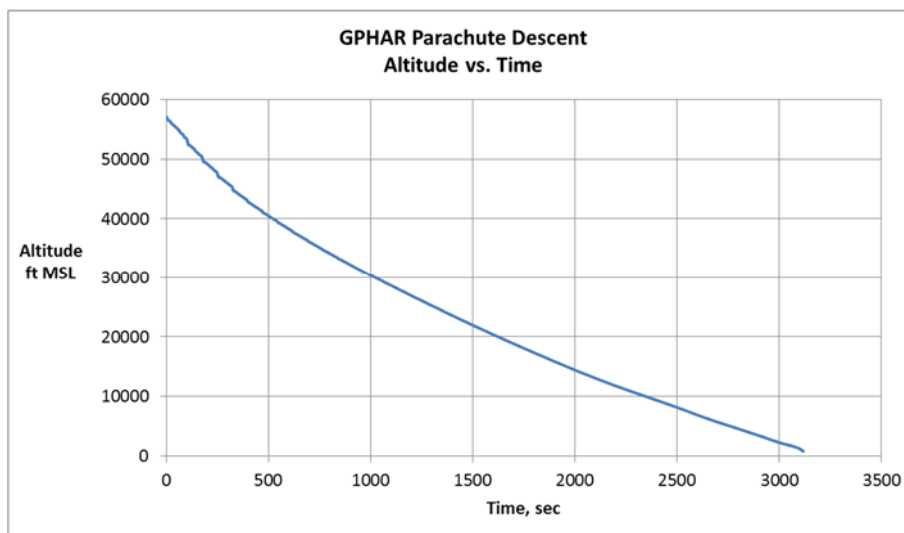


**Figure 16. Altitude Profile**

The wind heading observed during ascent and descent is shown in the figure below. During descent, the wind is calculated from heading differences between ground course and compass and using the known canopy forward airspeed. As would be expected, the lower altitude winds are slightly different between launch and landing locations. Comparing the system heading vs. altitude, it can be clearly seen the transition to autonomous occurs correctly at 12,000 ft. MSL. At this point, a heading is maintained to the northwest.

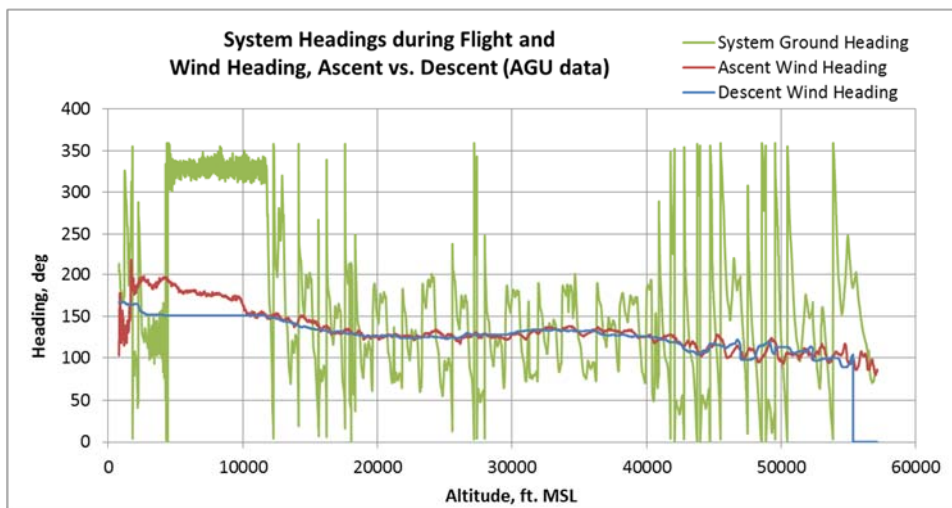


**Figure 17. System and Wind Headings**

#### **D. AGU Temperature Control**

Since the AGU is a critical component of any parafoil recovery system, a review of system performance was made. Besides the observation that all flight computer processes and data log files were observed to be nominal, the AGU was observed to have successfully endured the extreme environmental conditions associated with high altitude flight.

During flight, the AGU battery temperature was monitored and controlled by a thermal protection system. The ability of the AGU to maintain a higher operating temperature than the environment is seen with a comparison to

AGU and outside temperatures versus altitude. Note that during descent, the AGU temperature continued to drop, even though outside temperatures were increasing. This is likely due to wind chill effects. There are periodic temperature dropouts seen in the AGU temperature curve. These are believed to be artifacts of the sensor and are not instantaneous temperature changes since the thermal inertia of all of the internal components would make that impossible.

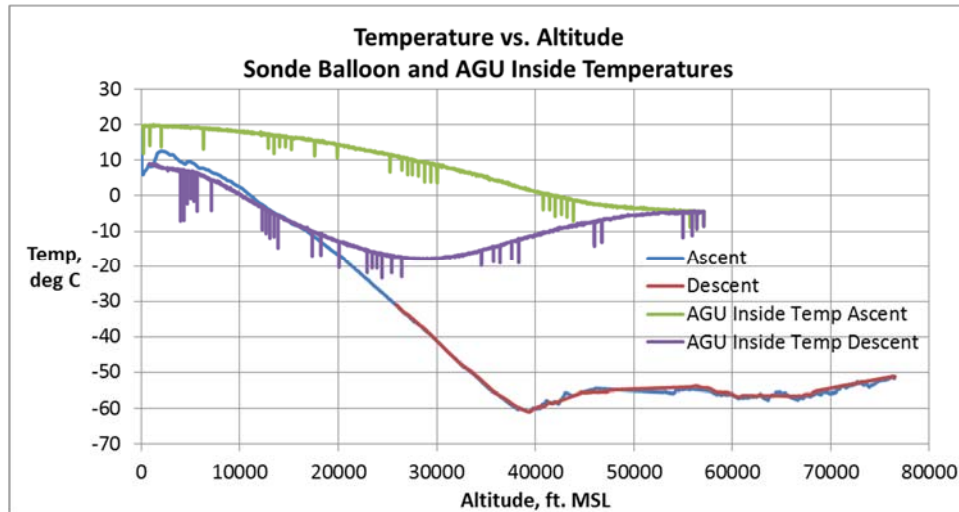


**Figure 18. Internal / External Temperature Comparison**

The thermal protection system was effective in maintaining the battery's current draw capabilities for the duration of the flight. The AGU performance on a whole (other than some communications) was nominal.

### E. Inflation

The inflation of the system was remarkably smooth. The energy attenuation strip activated after release of the canopy from the deployment bag and nicely prevented the parachute from rebounding into the payload, a big concern. The lines can be seen being pulled tight after rebound in the video. The system stopped accelerating after 280 ft. of descent. Forward flight experienced an overspeed condition before settling around 100 ft/s.

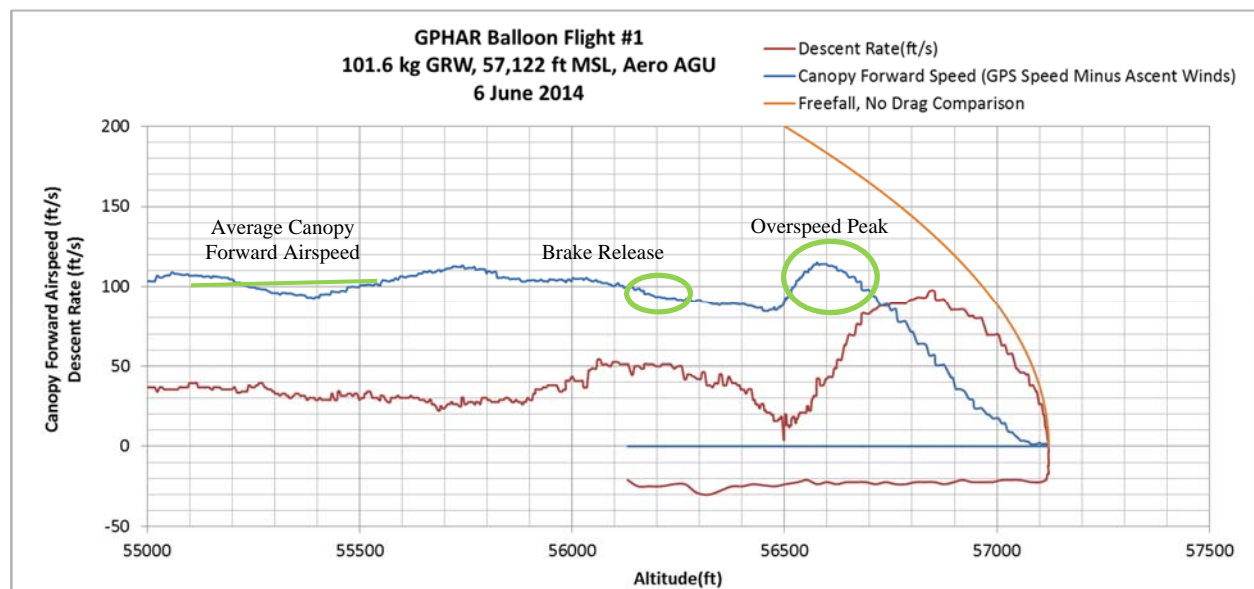


**Figure 19. Inflation Profile**

The inflation progression can be seen in the series of video screenshots below. The images begin just after NSC release. The deployment bag is seen at the center of the balloon with lines extending toward the payload. The deployment bag remains with the balloon. When the lines are fully paid out, one can see the lines get tight in the second image. This represents the line stretch / snatch event. After this event, the lines, acting like rubber bands, pull the parachute swiftly, accelerating the parachute in the direction of the payload, faster than the payload is falling. This is seen by the many slack and uncontrolled suspension lines in the third image. At this time, airspeed is very low and there is insufficient dynamic pressure to lift the parachute away from the payload.

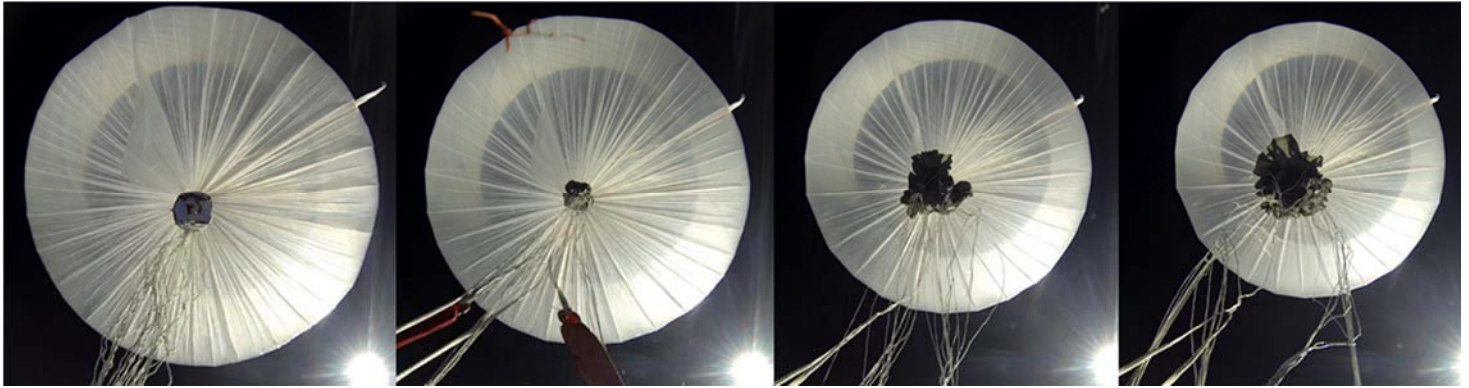
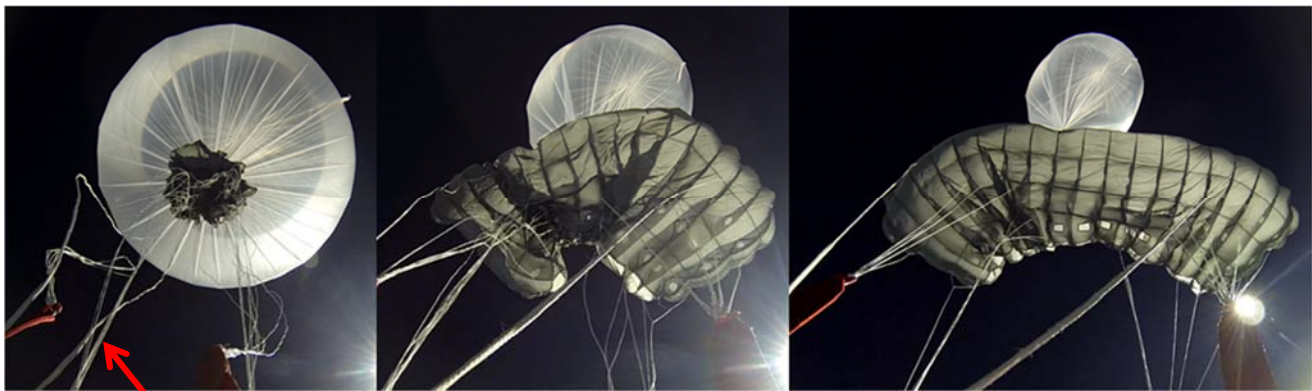


**Figure 20. Deployment Images thru Linestretch**

Shortly after the parachute exits the deployment bag, the attenuation strip activates. This is observed in the screenshot as front riser lines seen tight (attenuation strip does not tighten the rear riser lines). The other lines have significant slack, representative of a parachute that is trying to rebound toward the payload after the line stretch / snatch event. In the third image, the bottom skin of the canopy canopy is near full shape and lines have good continuity. The size of the balloon is an indicator in the amount of descent experienced.



Lines tight due to attenuation stitching

**Figure 21. Attenuation and Canopy Spreading**

These images show full planform dimensions of the bottoms skin and the beginning of parafoil pressurization, aided by eight square vents on the bottom skin. It is noticed that the center section inflates first due to these features.





**Figure 22. Initial Inflation**

The center cells are then pressurized, and the canopy continues to show good symmetry. In the second image, full pressurization is achieved and the wing is producing lift.



**Figure 23. Full Pressurization**

Since the system has zero initial horizontal velocity, the parachute must accelerate the payload to steady state canopy forward airspeed (about 100 ft/s). As a result of the direction of airflow, the parafoil lift vector is angled forward and the parachute surges and overflies the payload, resulting in producing more lift in the horizontal direction, helping to accelerate the payload to steady state canopy forward airspeed. The moment of surge is seen in the image below. Notice that the ground is visible in the upward facing camera.



**Figure 24. Canopy Surge (Predecessor to Overspeed Condition)**

Because the I230 surge and horizontal acceleration produced were so effective, the system actually experienced a momentary overspeed condition, with a horizontal velocity greater than the steady state. This then results in a pitch back of the canopy. In some systems, surging occurs several times before steady state is achieved. The I230 dampened quickly and experienced one large surge and one much smaller surge, with no heading changes.

This phenomenon is very common, and there was concern that the behavior of surging could have been detrimental at this altitude. Any changes in canopy heading during the surging could have produced undesirable results given the kinetic energy involved with the high canopy forward airspeeds. It was therefore critical to produce a symmetrical, on-heading opening, which was achieved.

## F. Velocities and Glide

Using the GPS ground speed and the wind profile recorded during the balloon ascent, the canopy forward airspeed of the system is calculated. The descent rate of the system is directly measured by the GPS. The ratio of canopy forward airspeed to descent rate represents the glide ratio, or “L/D” (L over D) of the system. The unfiltered performance data for the entire flight is seen below. Notable characteristics include large peaks and troughs in all three curves over about 35,000 – 40,000 ft. These are due to turns which above nominal descent rates followed by periods of below nominal descent rates in the recovery from the diving maneuver. In several instances, the recovery resulted in descent rates close to zero. The highest level flight achieved was 52,300 ft. This recovery behavior is natural and expected at low altitude, but it was not known if the ram air canopy would continue to behave this way at high altitude.

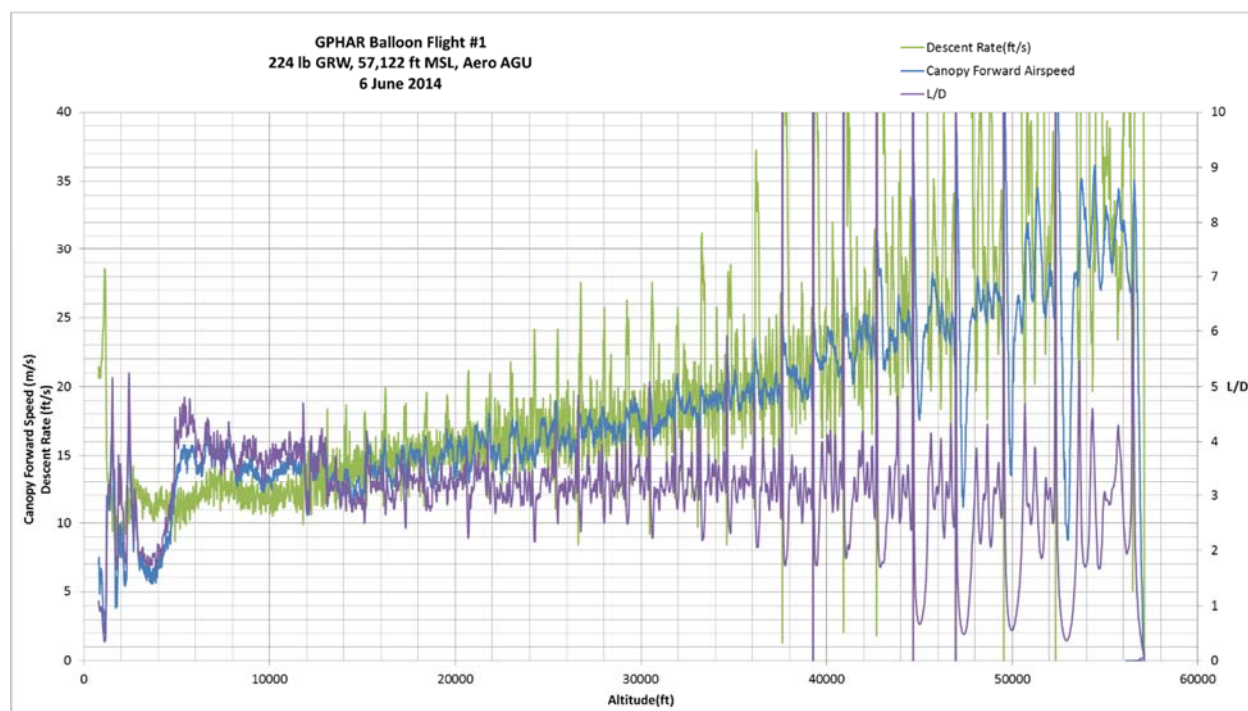


**Figure 25. GPHAR Forward Airspeed, Descent Rate, and L/D**

The glide ratio, over the data range 14,000 – 40,000 ft., is approximately 3.25 – 3.5. A slight dipping trend is noticed beginning at 40,000 ft., where the L/D average appears to lower to just about 3.0 at 55,000 ft., however the data is relatively dynamic during this time. It is reasonable to ignore the large spikes and troughs in L/D due to the R2 turn which entered dives until about 40,000 ft., which will be discussed further in subsequent sections. This characteristic is responsible for the majority of the large amplitude noise in the data.

Another notable observation is the high forward airspeed below 12,000 ft. The cause for this phenomenon is postulated to be due to differences between the actual real time wind conditions and the winds from the ascent used to calculate the forward airspeed. Wind below 13,000 ft. MSL near the landing location was substantially different than wind below 12,000 ft. MSL at the launch location. This presumption is supported by the large swing in GPS

speed below 5,000 ft. and the fact that it was observable in the onboard real time wind estimate by the AGU during the descent.

While the data of Figure 25 is very compressed and noisy, showing 52 minutes of flight and over 116 articulated turns, the parafoil was actually very stable. With the exception of R2 turns, after every turn was a prompt recovery and resumption of a stable steady state flight with parafoil solidly overhead. This is also very clear in the video of the descent. Some instances of periods of sustained descent rate precede turns in Figure 26. As a result of the excellent stability observed, this canopy provided discrete usable data on nearly each turn that was performed. Further, the canopy demonstrated all the desired characteristics necessary to be an autonomously controlled recovery system.

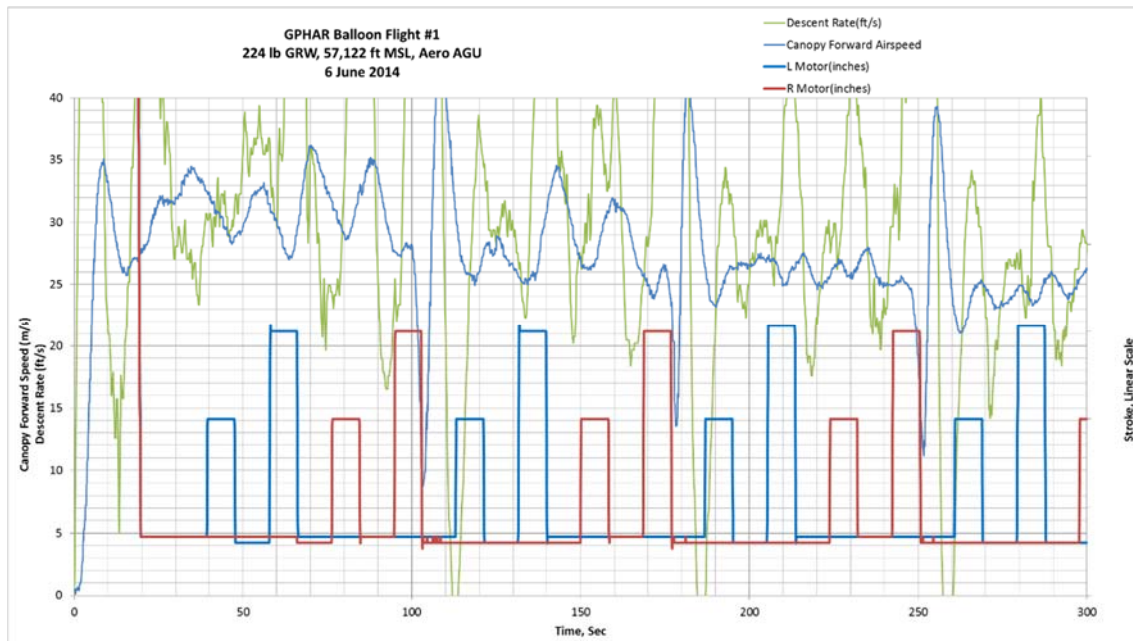


Figure 26. Speeds and Motor Positions above 45,000 ft.

### G. Turn Rates

The canopy was observed to have about a 3 deg/s turn rate to the right in full flight. This typically has the effect that right turns will be sharper than left turns, which was the case in flight. Near constant turn rates were observed in the left direction, but it can be seen that turn rates to the right diverge and are higher at altitudes above about 40,000 ft.

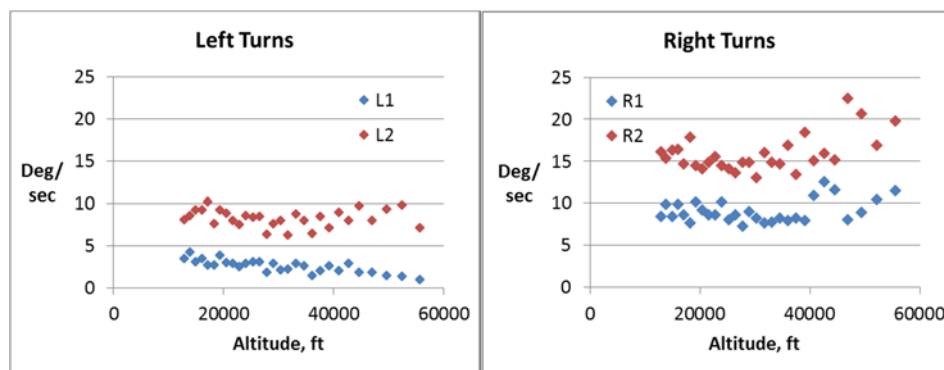


Figure 27. Turn Rates

An interesting observation was that while a diving turn was achieved for some large stroke inputs at higher altitudes, the turn rate was comparatively slower than low altitude diving turns, which can be well over 40 deg/sec. This was most easily recognized in watching videos. This behavior is a positive characteristic in that the dive could be more easily managed by the flight software. A negative characteristic is that a dive could be achieved with the reduced stroke which was used.



### H. Strokes and Accelerations

It is useful to compare the stroke timings with accelerations. A greater sensitivity to stroke inputs over about 40,000 ft. MSL is seen, which agrees with the spiking of GPS speed and descent rates in previous sections. The largest responses occurred for the R2 turn, the large turn in the direction of the bias. Accelerations of approximately 2.75 g's are experienced during / after diving turns.

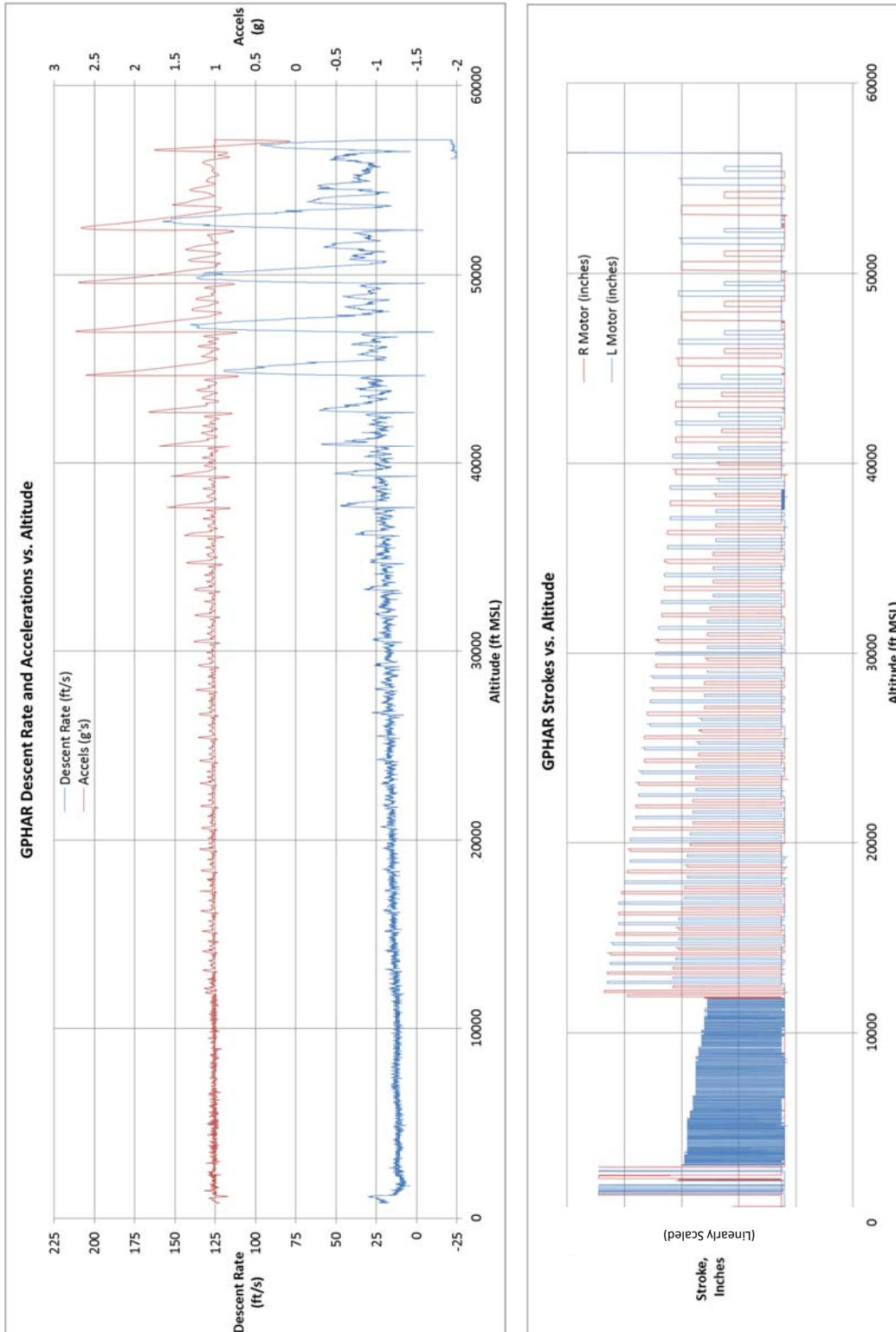


Figure 28. Choreographed Comparison between Stroke Input, Descent Rate, and Accelerations



All stroke inputs were held the same amount of time. The difference in stroke column width at higher altitudes is due to differences in descent rate due to air density, but also, and perhaps even more so, the amount of altitude consumed during the turn. It can be seen that the width of the R2 turns, as well as the width of the full flight gap between R2 and L1, are much wider than others, especially above 40,000 ft., where diving spiral turns were experienced. After a diving turn, the descent rate can be seen to be negative momentarily, indicating straight and level flight is possible by parafoil parachutes at these altitudes.

Below 12,000 ft., many small left motor inputs can be seen. These are periodic small left turn inputs which are commanded to counter the right bias experienced, and are representative of the flight software operating correctly.

## V. System Analysis

### A. Evaluation of Observed vs. Expected Velocity

The GPS speed minus wind was further manipulated to have data affected by turns removed and data below 12,000 ft. removed. The canopy forward airspeed over the altitude range indicated shows good agreement with a theoretical speed based on air density alone if L/D were fixed, however there is a noticeable deviation beginning around 45,000 ft.

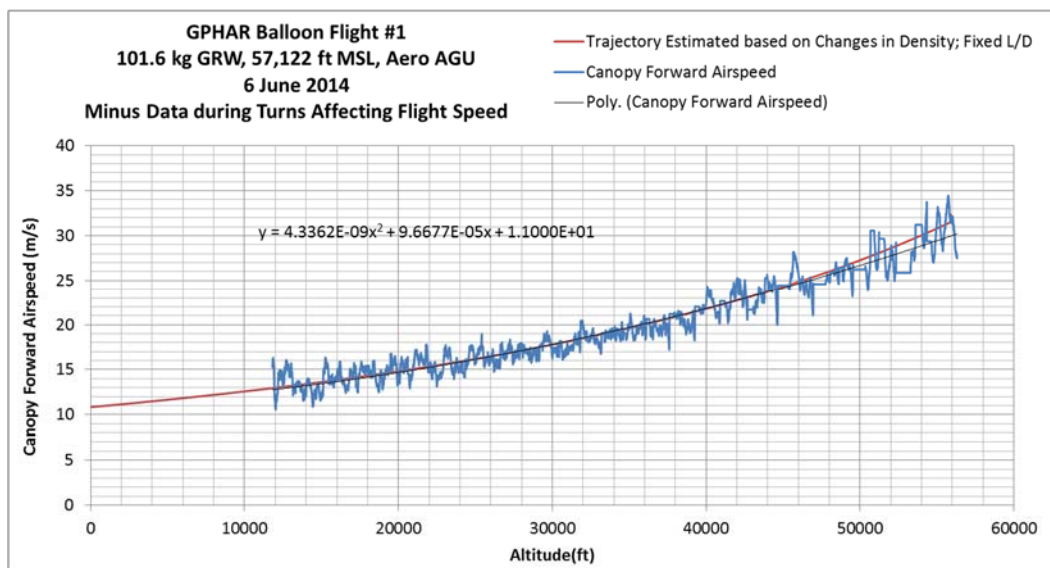
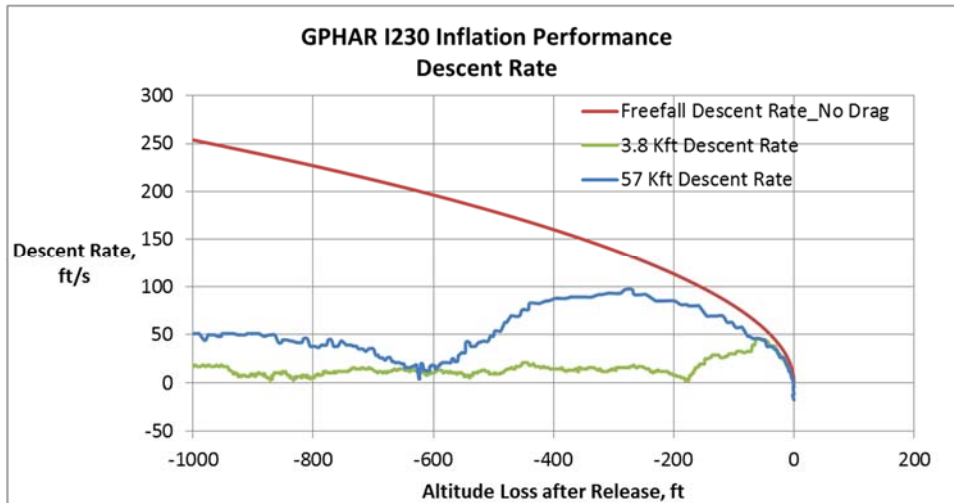


Figure 29. Canopy Forward Speed Profile

It is noted that the GPS speed is a little slower than theoretical at high altitudes. This could be due to the more dynamic behavior observed above 40,000 ft. All efforts were made to only include data during periods of steady flight, so this effect should be reduced. This involved cropping data during and after the R2 turns at altitudes down to about 35,000 ft. This could also be due to changes in lift and drag coefficients of the parafoil due to Reynolds Number, discussed later.

### B. Comparison to Low Altitude Performance

This can be compared with an earlier test of the same deployment train at 3,800 ft. MSL, which showcases the difference due to air density. In GPHAR Flight 1, the maximum descent rate was about 97 ft/s after a loss of 280 ft. In the low altitude release, the max descent rate was 45 ft/s with a loss of 58 ft. After 1,000 ft. of descent, with both at steady state, the descent rate of GPHAR is about 3 times faster at 57 kft.



**Figure 30. Inflation Performance – Descent Rate**

For added perspective, the negative descent rate of the climb of the balloon is shown, as well as a curve of a freefalling body with no drag. While not clearly visible, the 3,800 ft. release started with an existing approximately 15 ft/s descent rate due to the host platform. Both descent rate curves show a similar characteristic hump after release of a period with higher than steady state descent rate, followed by a lower than steady state descent rate, and then steady state. The 57 kft. curve, however, has a much broader curve and extends to higher descent rates, as would be expected.

The 57 kft. release was accelerating the first 275 ft. of descent and achieved steady state at approximately 800 ft. of descent, where the 3,800 ft. release required approximately just 250 ft. Note that an ascending release occurred on the 57 kft. flight (22 ft/s) and a descending release occurred on the 3,800 ft. flight (-15 ft/s).

The difference in canopy forward airspeed also show the expected trend of higher peak and protracted curve. The steady state speeds were also about 3 times faster after 1,000 ft. descent. The wind as observed on the 3,800 ft. flight at the time of release was subtracted from the GPS speed to get canopy forward airspeed. Both curves have had wind effects removed. The magnitude of the speed therefore has some error but the timing of overspeed and damp out is accurate.

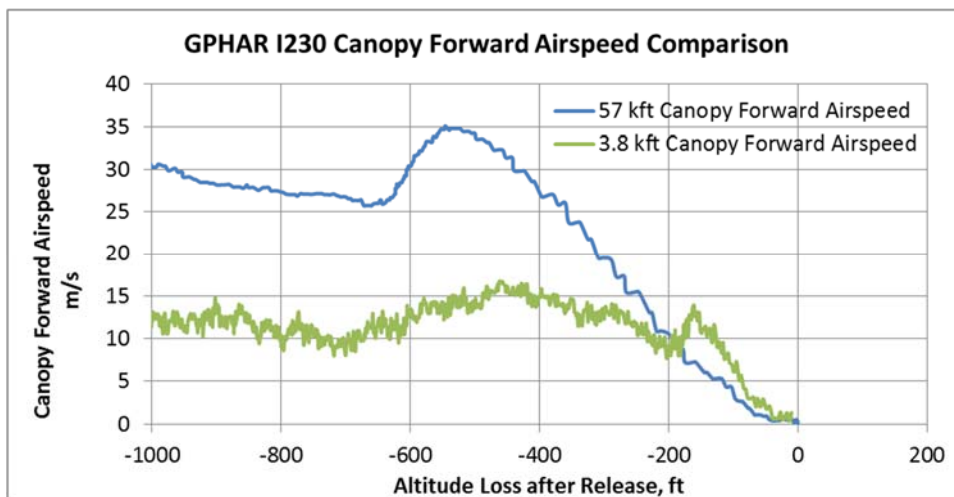


**Figure 31. Comparison of Canopy Forward Airspeeds**

Combining the descent rate and canopy forward airspeed onto one plot and comparing against timed events, the reactions to control inputs can be observed. Turn markers represent the beginning of a turn stroke, which is held for 8 seconds.

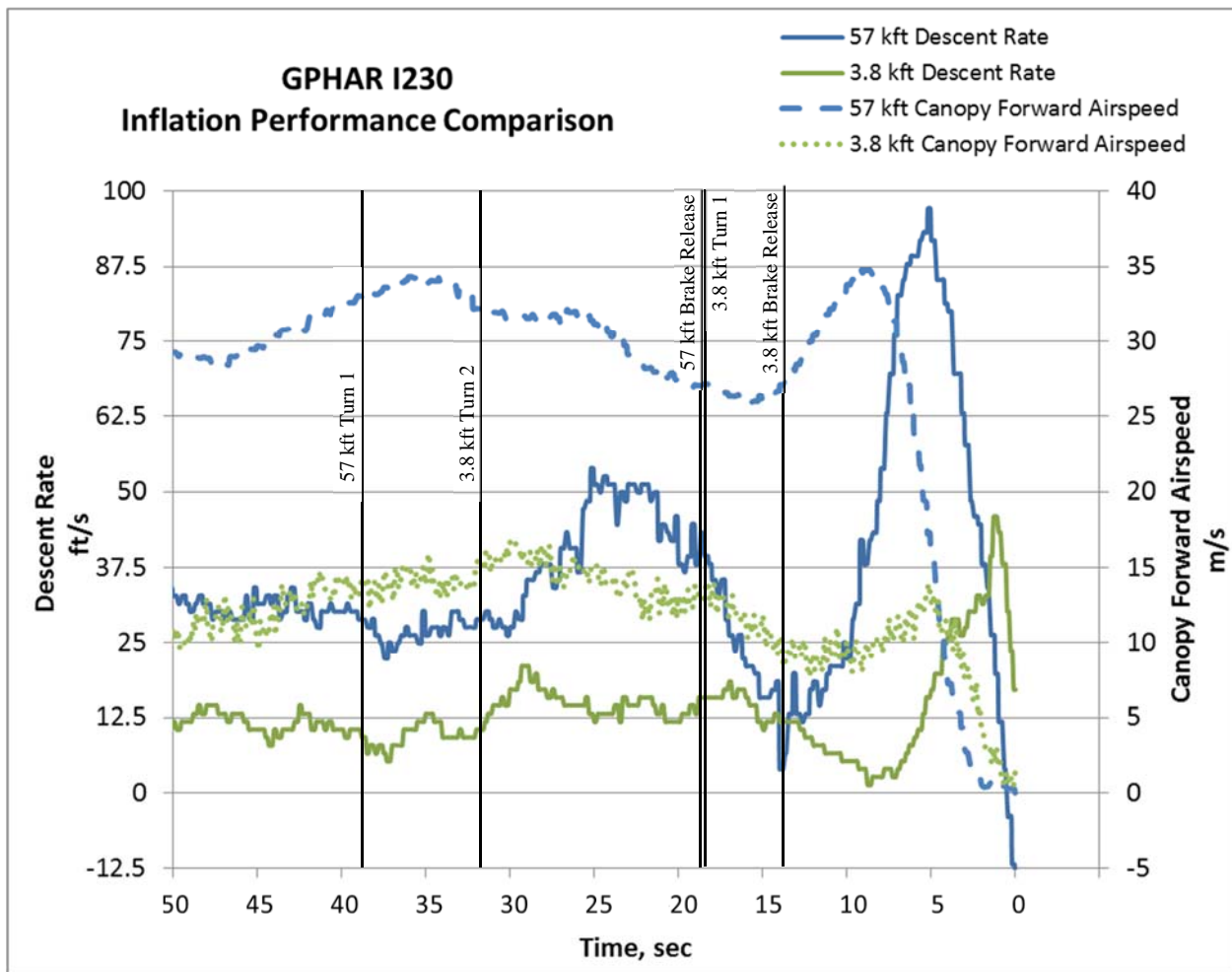


**Figure 32. Inflation Performance Summary with Time Events**

Both descent rate and canopy forward airspeed increase after brake release, which is to be expected. The steady state values of each are higher than with the brakes stowed. In the turns shown above, a dive was not achieved. Had a dive been achieved, the canopy forward airspeed would not have been calculated correctly, since this value is based on horizontal travel based on latitude and longitude GPS values.

### C. Reynolds Number Considerations for Future Developments

With the airspeed data collected, the Reynolds Number for altitudes flown can be plotted. While there was no concern for the GPHAR test that was conducted, it is interesting to continue the curve to even higher altitudes based on an estimated L/D of a constant value. Due to consequences of low Reynolds Numbers, some applications at potentially much higher altitudes, up to 130,000 ft., may have concern.

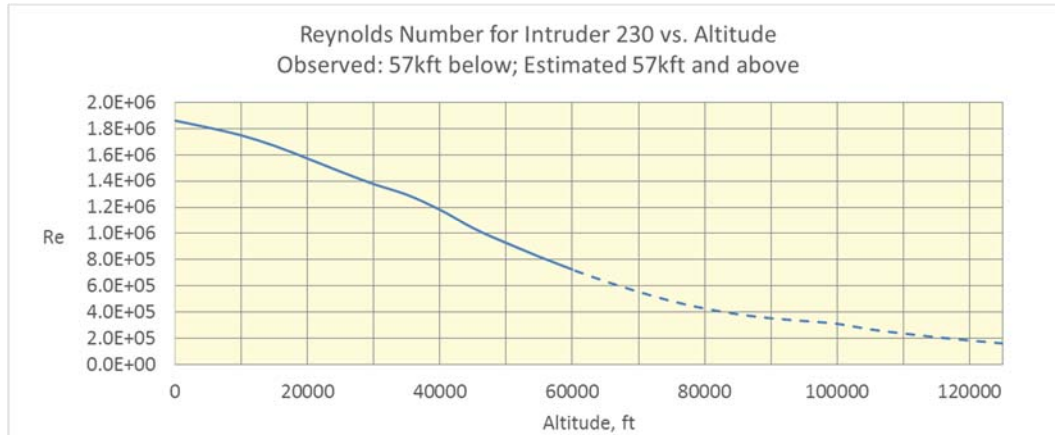


**Figure 33. GPHAR Actual and Theoretical Reynolds Numbers**

As Reynolds Numbers decrease below  $10^6$ , the L/D for published root airfoil sections are commonly known to decay, example being Selig<sup>3</sup>. The lift coefficient and drag coefficient are both observed to shift, each with negative consequence to L/D. At Reynolds Numbers below  $2 \times 10^5$ , which corresponds to 120,000 ft. MSL, the impact to L/D could be more than half.

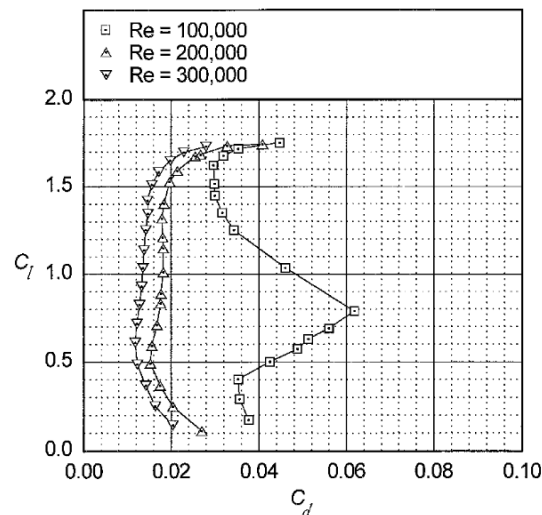


**Figure 34. Example Lift-Drag Polar at Different Re, for FX 63-137 Airfoil (Selig)**

It is uncertain what effect this would have on an inflated parafoil parachute, which resembles the root airfoil section very poorly. Small parafoil canopies, with a chord of 2-3 ft., that fly with true airspeeds below around 30 ft/s, could encroach on these low Reynolds Numbers. Experiments with small parafoils could be an interesting area to investigate economically.

### D. Mach Considerations for Future Developments

The maximum true airspeed experienced by the GPHAR system was approximately 200 ft/s at about 53,000 ft. MSL, or about Mach 0.2. This occurred during the first R2 turn. Had this turn occurred after release from 130,000 ft., assuming parafoil performance extrapolates to these altitudes, the speed would have been approximately 760 ft/s

or Mach 0.76. At Mach numbers greater than about 0.3, subsonic compressibility flow occurs, which currently has unknown impacts on a parafoil parachute.

### **E. MOI Considerations for Future Developments**

For a parafoil parachute, the yaw and roll MOI's would be dependent on the mass of the fabric cloth, the lines, and the apparent mass of the air contained inside the cells. For the GPHAR canopy, the internal volume is approximately 103 ft<sup>3</sup>, which would correspond to about 8 lbs of air mass at sea level. Given the mass of the parachute, at very high altitudes, say 130,000 ft., this would reduce the MOI of the parachute system by almost half, making it easier for the parafoil to roll or yaw.

## **VI. Summary / Conclusion**

The research conducted under the GPHAR program has yielded significant findings that will aid the further development of parafoil parachutes for space access recovery applications. Primary findings have included:

- Parafoil deployment via static line is a viable method of deployment up to 57,000 ft. for parafoils of around 230 ft<sup>2</sup>
- On attainment of steady state full flight
  - Steady state was achieved without significant surging or cycles of surging
  - The parafoil recovered quickly following turns
  - The descent rate and canopy forward airspeed possessed the same progression characteristics as in lower altitude inflations
- Flight at these altitudes proved stable and controllable
- Parafoil turn responses were within the realm of AGU flight software handling capabilities
- The AGU effectively provided control inputs and recorded flight data at the higher altitude environments
- L/D began to show a minor decay at about 45,000 ft., where the Reynolds Number approached  $8.3 \times 10^5$  (steady state full flight)
- The ability to achieve level flight was temporarily achieved following a diving R2 turn at 55,000 ft. The ability to achieve level flight is likely possible at much higher than 55,000 ft., especially with control input.
- The stroke scaling technique was effective in safely allowing turn observations at high altitudes. The strokes used would be appropriate for real applications at these altitudes.

Additionally, the research has allowed the collection of lessons learned, recommendations for future work, and next steps.

### **A. Lessons Learned**

Overall, the ram air canopy deployment was very clean and orderly and canopy flight performance was quite close to prior experience. These observations confirm that parafoil parachutes maintain flight and glide performance throughout the altitude envelope experienced, an application relevant environment, which provides entry into TRL 5, "System validation in relevant environment". These results are fully expected to be reliable and repeatable, leaving doors open for high altitude recovery using parafoils of this size and payloads of this weight.

This test provided crucial information about an unknown phenomenon concerning parafoil canopies that have high sensitivity to very small stroke inputs above 40,000 ft. This phenomenon can be expected for a wing loading of approximately 1:1, as tested. Data was collected showing very small strokes are capable of diving turns.

If bias were not experienced, it is expected that the hard dives would not have been experienced, or at least much reduced from their current form. However, diligence should be used to plan and design for tolerance to turn bias.

Concerning navigation and control, the test provided critical data that suggests, while the nature of the maneuvering dynamics are consistent with low altitude flight, the recovery time from a maneuver is longer at high altitude. This must be accounted for in the guidance, navigation, and control logic. A neutral command position (i.e. no inputs) should be used for at least 10-12 seconds following a large stroke input. This will allow the system to dampen out non-steady kinetics and resume steady state flight. No turns should be commanded during any times with accelerations greater than about 1.1 g. Also, strokes should not be held for extensive durations (greater than 360 degree turn) due to the phenomenon of spiral divergence (i.e. a turn maneuver devolving into a dive). Note that this behavior is also consistent with ram air canopy performance at low altitude.

## B. Recommendations

Concerning future parafoil system applications, which could operate up to 130,000 ft. MSL, some of the following concepts may be appropriate to consider:

- Turns should be made only when required for heading correction or proximity containment; the fewer turns, the better
- Only the L1 / R1 small strokes should be used
- Strokes for higher altitudes should probably be reduced still, extrapolated from the current scaling law
- Wind tunnel tests or drop tests of a small scaled parafoils at Reynolds Numbers that have yet to be flown or documented. An objective would be to understand how compressibility affects parafoils and also when and how L/D decays
- Search out and implement a higher altitude capable GPS
- For future applications it is recommended to use a parafoil planform with low sensitivity to control inputs to achieve control while minimizing stability issues; lower aspect ratio planforms may be controlled more easily

## C. Technology and Next Steps

Due to weather restrictions and schedule availability, only 1 of the 3 planned balloon drop tests has occurred thus far during this phase of the GPHAR Flight Opportunities Program. Future exploratory drop tests of GPHAR or other development programs should aim to further extend the TRL of high altitude parafoil recovery, and should include next step efforts of:

- Demonstrate fully autonomous navigation for entirety of flight profile
  - Achieve the ability to acquire and maintain headings in desired directions
  - Consistent and controllable system response across the descent profile
  - Precision landing at designated landing point from maximum standoff.
- Higher altitudes – potential to match Mars densities
- Higher airspeed (descent rate) at time of main canopy inflation; use of slider reefing device
- Higher and lower wing loading of the ram air canopy
- Larger parafoil parachutes
- Increased instrumentation (additional video angles, airspeed measurement device etc.)
- Demonstrate high altitude mission planning; autonomous downselection of a suitable landing site based on proximity to pre-selected acceptable landing points

## VII. Acknowledgements

Airborne Systems would like to thank NASA and Near Space Corporation for their support of this flight opportunity. The flight test achieved was a major success and represents a significant advancement in the state of the art of ram air parachute technology. We look forward to the opportunity for additional drop tests in the future via recycling or a new phase of the FOP.

## VIII. References

<sup>1</sup> Fields, T., Yakimenko, O., “Lower Stratospheric Deployment Testing of a Ram-Air Parafoil System,” 2014 AIAA Atmospheric Flight Mechanics Conference, AIAA 2014-0193.

<sup>2</sup> Mckinney, J., Lowry, C., “Mars Precision Landing Using Guided Parachutes,” 20<sup>th</sup> AIAA Aerodynamic Decelerator Systems Technology Conference, AIAA 2009-2983.

<sup>3</sup> Selig, S., Guglielmo, J., “High-Lift Low Reynolds Number Airfoil Design,” Journal of Aircraft, Vol. 34, No. 1, 1997.

<sup>4</sup> Lingard, J., “Ram-Air Parachute Design,” Precision Aerial Delivery Seminar, 13<sup>th</sup> AIAA Aerodynamic Decelerator Systems Technology Conference, 1995.

<sup>5</sup> AFFDL-TR-78-151, “Recovery Systems Design Guide,” Dec 1978, Air Force Flight Dynamics Laboratory.

<sup>6</sup> Knacke, T., “Parachute Recovery Systems,” NWC TP 6575, Para Publishing, 1992.